




# Characterization of two orthologs of bacterial intramembrane metalloprotease RseP by native mass spectrometry

Michiko Tajiri<sup>1</sup> · Tomoya Shida<sup>1</sup> · Rika Oi<sup>1</sup> · Hinako Kondo<sup>1</sup> · Keiko Shimamoto<sup>2</sup> · Yukinari Kato<sup>3</sup> · Terukazu Nogi<sup>1</sup> · Satoko Akashi<sup>1</sup> 

Received: 2 April 2025 / Revised: 28 September 2025 / Accepted: 7 October 2025  
© The Author(s), under exclusive licence to Springer-Verlag GmbH, DE part of Springer Nature 2025

## Abstract

Intramembrane metalloproteases are conserved in all three domains of life and regulate cellular signal transduction by cleaving membrane-anchored precursors or regulators of transcription factors. Bacterial intramembrane metalloproteases are promising targets for antimicrobial drugs as they are implicated in pathogenicity and drug resistance. Understanding the properties of intramembrane metalloproteases, particularly their interactions with zinc and inhibitors, is important for drug development. While native mass spectrometry (MS) is effective for studying intermolecular interactions, its application to membrane proteins, including intramembrane metalloproteases, presents a unique challenge for preserving noncovalent interactions in the gas phase due to their hydrophobic nature. In this study, we utilized native MS to investigate zinc and inhibitor binding to two bacterial intramembrane metalloproteases, *Escherichia coli* RseP (*EcRseP*) and its ortholog from *Kangiella koreensis* (*KkRseP*). Intact protein ions were successfully observed following optimized purification and buffer exchange protocols. Native MS revealed zinc binding to both orthologs, with *EcRseP* exhibiting higher affinity. In the presence of batimastat, a specific *EcRseP* inhibitor, both RseP orthologs formed stable complexes, demonstrating batimastat binds exclusively to zinc-bound RseP. These results demonstrate the ability of native MS for characterizing membrane protein interactions and highlight its potential as a platform for identifying specific binding events, thereby extending its established application with soluble proteins.

**Keywords** Native mass spectrometry · Membrane proteins · Protein–inhibitor complex · Bacterial intramembrane protease · Metal binding

## Introduction

Membrane proteins are critical mediators of signal transduction between intracellular and extracellular environments. Intramembrane proteases, evolutionarily conserved

from bacteria to humans, play a central role in this process [1–3]. Upon signal perception, these proteases cleave substrate proteins/peptides, releasing signaling molecules, such as transcription regulators and secreted proteins, from the membrane [1–3]. Bacterial RseP, an intramembrane metalloprotease found in the *Escherichia coli* (*E. coli*) inner membrane, is implicated in the extracytoplasmic stress response and the removal of remnant signal peptides from secreted proteins [4–9]. RseP-mediated proteolysis is vital for *E. coli* survival, and its deletion is lethal [4]. Furthermore, RseP homologs in bacterial pathogens have been implicated in infection and persistence, leading to the development of multidrug resistance [10]. Consequently, understanding the mechanism of RseP function is crucial for the development of antimicrobial drugs targeting intramembrane metalloproteases in pathogenic bacteria. Based on this strategy, we previously determined the crystal structures of *E. coli* RseP (*EcRseP*) and *Kangiella koreensis* RseP (*KkRseP*)

Michiko Tajiri and Tomoya Shida contributed equally to this work.

✉ Satoko Akashi  
akashi@yokohama-cu.ac.jp

<sup>1</sup> Graduate School of Medical Life Science, Yokohama City University, 1-7-29 Suehiro-Cho, Tsurumi-Ku, Yokohama, Kanagawa 230-0045, Japan

<sup>2</sup> Suntory Foundation for Life Sciences, 8-1-1 Seikadai, Seika-Cho, Soraku-Gun, Kyoto 619-0284, Japan

<sup>3</sup> Department of Antibody Drug Development, Tohoku University Graduate School of Medicine, 2-1 Seiryō-Machi, Sendai, Miyagi 980-8575, Japan

complexed with inhibitors, providing valuable structural insights [11].

In the present study, we utilized native mass spectrometry (MS) to characterize zinc and inhibitor binding to two bacterial RseP orthologs, *EcRseP* and *KkRseP*, because native MS is a promising platform for characterizing noncovalent interactions [12–15]. For example, we previously demonstrated its ability to selectively identify methotrexate, a specific inhibitor of dihydrofolate reductase (DHFR), from a mixture of eight candidate compounds, even in crude environments [16]. While native MS has been successfully applied to soluble proteins, the analysis of membrane proteins presents distinct challenges. Typically, membrane proteins are solubilized in micelles, purified, and then analyzed using MS [17, 18]. Although the molecular mass of an intact protein can be determined by removing only the micelle components during native MS, this process often requires substantial energy input. Minimizing energy input is crucial to prevent protein denaturation. Consequently, detergents with lower stabilizing abilities, while disadvantageous for purification, are preferred for native MS [19]. To address this inherent conflict, membrane proteins are often purified using highly stabilizing detergents and subsequently subjected to detergent exchange for a more easily removable detergent prior to MS [20]. Furthermore, harsh MS conditions can compromise membrane protein integrity, hindering the acquisition of native mass spectra. Maintaining intact membrane protein–drug complexes during native MS requires meticulous optimization of sample preparation and measurement conditions, making this analysis particularly challenging [21–23].

Although challenging, this study investigated zinc and inhibitor binding to bacterial intramembrane metalloprotease RseP orthologs, *EcRseP* and *KkRseP*, using native MS. The crystal structures of these proteins have been determined only for the inhibitor-bound forms [11]. Following expression and purification of these two proteins from an *E. coli* overexpression system, we optimized detergent conditions for native MS. We then explored native MS parameters for both intact RseP and RseP–inhibitor complexes. Through rigorous experimentation, we successfully characterized these orthologs using native MS. Considering prior biochemical analyses that revealed differences in protease activity between these RseP orthologs [11], we also discuss their behavior in native MS and the relationship to their enzymatic activity.

## Materials and methods

### Chemicals

The detergent [G1]-ether-C12 (G1) was synthesized as previously reported [23, 24]. Sucrose monolaurate (SM) and *n*-dodecyl-*N,N*-dimethylamine *N*-oxide (DDAO) were

purchased from Anatrace (Maumee, OH). Tetraethylene glycol mono-octyl ether (C8E4) was obtained from Sigma-Aldrich (St. Louis, MO). All the other chemicals were purchased from Nacalai Tesque (Kyoto, Japan).

### Preparation of *EcRseP*

*EcRseP* was prepared basically as described previously [11]. Briefly, the DNA sequence encoding *EcRseP*, fused to a C-terminal sequence containing a TEV cleavage site, His<sub>8</sub>-tag, Myc epitope, and PA-tag, was inserted into a pUC118-based plasmid, designated pNY1452. Protein sequences are shown in Figure S1. The plasmid pNY1452 was transformed into *E. coli* C43(DE3) (Lucigen, Middleton, WI), and *EcRseP* expression was induced by 0.5 mM isopropyl-β-D-1-thiogalactopyranoside (IPTG). *E. coli* cells were cultured in LB medium [Bacto Tryptone (10 g/L), yeast extract (5 g/L), and NaCl (10 g/L), without pH adjustment] at 30 °C for approximately 3.5 h. The cells were harvested and sonicated in 20 mM Tris–HCl (pH 7.4), 150 mM NaCl, and 0.1 mM 4-(2-aminoethyl)benzenesulfonyl fluoride hydrochloride (AEBSF) on ice. The lysate was centrifuged at 8400 *g*, and the supernatant was ultracentrifuged at 200,000 *g* at 4 °C. The membrane fraction (pellet) was resuspended in 20 mM Tris–HCl (pH 8.0), 150 mM NaCl, and ultracentrifuged again at 257,000 *g* at 4 °C. The resulting membrane pellet was resuspended in 20 mM Tris–HCl (pH 8.0), 150 mM NaCl, and mixed with an equal volume of 20 mM Tris–HCl (pH 8.0), 150 mM NaCl, 10% glycerol, 0.1 mM AEBSF, and 2% SM to solubilize the protein. The protein was purified by affinity chromatography using Sepharose resin conjugated to the NZ-1 antibody, specific for the PA-tag sequence (GVAMP-GAEDDVV) (PA tag system). Elution of *EcRseP* was performed with 20 mM Tris–HCl (pH 8.5), 150 mM NaCl, 10% glycerol, 5 μM Zn(OAc)<sub>2</sub>, 0.032% SM, and 0.1 mg/mL PA12 peptide (GVAMPGAEDDVV). Eluted fractions were collected, and the C-terminal tag region was removed by TEV protease digestion. Tag-removed *EcRseP* was purified by size-exclusion chromatography using a Superdex 200 Increase 10/300 GL column (Cytiva, Marlborough, MA). The protein was eluted with 20 mM Tris–HCl (pH 8.5), 150 mM NaCl, 10% glycerol, 5 μM Zn(OAc)<sub>2</sub>, and 0.032% SM.

### Preparation of *KkRseP*

*KkRseP* was produced as a PA-tagged protein. Briefly, the DNA sequence encoding *KkRseP*, fused to a C-terminal tag containing a Myc epitope and PA-tag, was inserted into an expression plasmid. Protein sequences are shown in Figure S1. The prepared plasmid, designated pNY1459, was transformed into *E. coli* C43(DE3), and *KkRseP* expression was induced with 0.5 mM IPTG. *E. coli* cells were cultured in LB medium at 15 °C for approximately 18 h. Cells were harvested and

sonicated in 20 mM Tris–HCl (pH 7.4), 150 mM NaCl, and 0.1 mM AEBSF on ice. The lysate was centrifuged at 8400 *g*, and the supernatant was ultracentrifuged at 200,000 *g* at 4 °C. The membrane fraction (pellet) was resuspended in 20 mM Tris–HCl (pH 8.0), 150 mM NaCl, and was ultracentrifuged again at 257,000 *g* at 4 °C. The resulting membrane pellet was resuspended in 20 mM Tris–HCl (pH 8.0), 300 mM NaCl, 10% glycerol, and 0.1 mM AEBSF, and mixed with an equal volume of 20 mM Tris–HCl (pH 8.0), 300 mM NaCl, 10% glycerol, 0.1 mM AEBSF, and 2% SM to solubilize the protein. The protein was purified by affinity chromatography using the PA-tag system. Elution was performed with 20 mM Tris–HCl (pH 8.0), 300 mM NaCl, 10% glycerol, 5  $\mu$ M Zn(OAc)<sub>2</sub>, 0.032% SM, and 0.1 mg/mL PA12 peptide. Eluted fractions were collected, and *KkRseP* was further purified by size-exclusion chromatography using a Superdex 200 Increase 10/300 GL column. The protein was eluted with 20 mM Tris–HCl (pH 8.0), 300 mM NaCl, 10% glycerol, 5  $\mu$ M Zn(OAc)<sub>2</sub>, and 0.032% SM.

### Native mass spectrometry of RseP orthologs

For native MS measurements, the freshly prepared protein solution was exchanged into 200 mM ammonium acetate (pH 7.4) containing DDAO, G1, or C8E4 using Micro Bio-Spin™ 6 columns (Bio-Rad, Hercules, CA) [19]. The detergent concentration was set to 2× or 3× CMC for DDAO and C8E4, and equal to the critical aggregation concentration (CAC) for G1. The concentrations of protein samples were measured after buffer exchange. To prepare protein solutions with different concentrations, the protein samples were serially diluted, and the resulting solutions were subjected to native MS. The protein solution was then loaded into in-house prepared nanoelectrospray (nanoESI) emitters with an inner diameter of approximately 3  $\mu$ m, and the emitters were placed in a nanoESI source on a SYNAPT G2 HDMS mass spectrometer (Waters, Milford, MA). We optimized the capillary voltage (0.68–1.0 kV) and collision voltage (25–60 V) to find the optimal conditions for each detergent. Subsequently, the mass spectra were measured using the parameters listed in Table S1. The sampling cone voltage was set to 40 V, ion source temperature was 70 °C, Ar gas flow rate was 3.0 mL/min, and backing pressure in the source region was 5.0–5.5 mbar. The mass spectra were processed using MassLynx v.4.2 software.

## Results and discussion

### Detergent selection for RseP native MS

In the established purification protocol of recombinant RseP proteins for X-ray crystallography, *EcRseP* is purified in 0.05% SM micelles, while *KkRseP* is purified in 0.03% dodecylmaltoside (DDM)/0.006% cholesterol

hemisuccinate (CHS) micelles, both conferring high stability and functional preservation [11]. However, native MS requires micelle removal, which may compromise protein integrity, particularly for membrane protein–drug complexes. This presents a challenge: crystallography favors detergents that tightly bind and stabilize the protein, whereas native MS demands easily removable detergents, including DDAO, C8E4, and G1 (Figure S2). Initially, we attempted native MS of *EcRseP* in SM micelles and *KkRseP* in DDM/CHS micelles after the micelle exchange to native MS compatible detergents. However, *KkRseP* in DDM/CHS micelles exhibited resistance to exchanges into DDAO, G1, or C8E4. This might have resulted due to differences in micelle size, as DDM micelles are larger than SM, and DDAO micelles are significantly smaller [19, 25, 26]. This suggests that transitioning from larger to smaller micelles is energetically unfavorable. Consequently, *KkRseP* was purified in SM micelles in a similar manner to *EcRseP* to facilitate compatibility with native MS.

In the present study, both *EcRseP* and *KkRseP* prepared in the buffer with SM underwent buffer exchange using size-exclusion spin columns into 200 mM ammonium acetate solutions containing DDAO, G1, or C8E4 for subsequent MS analysis. DDAO is a zwitterionic surfactant characterized by a long C12 hydrophobic carbon chain with a zwitterionic head group. C8E4 is a nonionic surfactant consisting of a C8 hydrophobic carbon chain linked to a tetraethylene glycol head group. G1 is also a nonionic surfactant, designed and developed as an ideal detergent for the native mass spectrometry of membrane proteins, featuring a C12 hydrophobic carbon chain linked via an ether oxygen to a branched ethylene glycol head group. As shown in Fig. 1, DDAO yielded high signal-to-noise ratios (S/N) mass spectra for both *EcRseP* and *KkRseP* at approximately 2  $\mu$ M. In contrast, C8E4 micelles resulted in the lowest quality spectra. The optimal sampling cone voltages and collision voltages varied among the detergents, with C8E4 requiring the highest energy input (Table S1). This suggests that the elevated energy required for C8E4 removal may have contributed to RseP degradation. While G1, a detergent specifically designed for membrane protein analysis in native MS [24], previously demonstrated superior performance for intact  $\beta_2$ AR [23], DDAO proved to be more effective for RseP analysis in this study. This discrepancy underscores the protein's specific nature of detergent selection for native MS, emphasizing the absence of universal rules [27].

### Zinc binding to RseP orthologs

A zinc ion, essential for RseP protease activity, is located within the active site [11]. However, due to its inherent

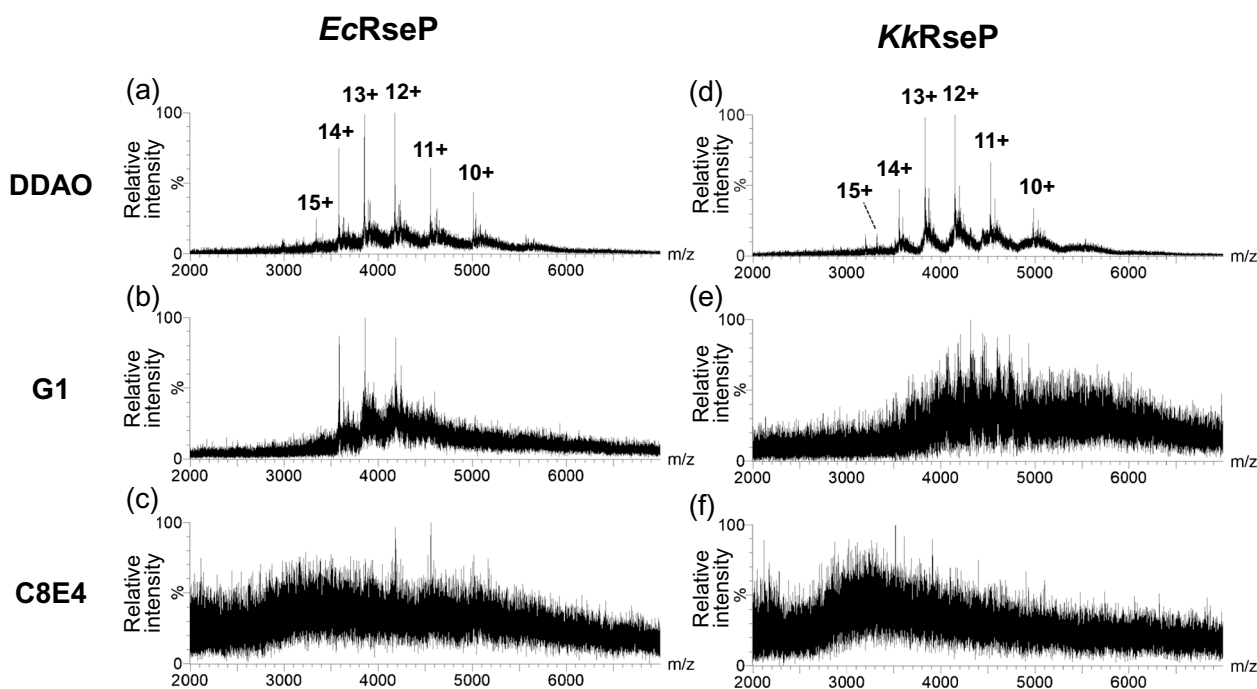


**Fig. 1** Native mass spectra of *Ec* and *Kkr*RseP. Samples were prepared in 200 mM ammonium acetate (pH 7.4) containing DDAO (a, d), G1 (b, e), or C8E4 (c, f), respectively

instability, the structure of the two RseP orthologs in the absence of an inhibitor remains undetermined. In the mass spectra shown in Fig. 2, both RseP orthologs retained a zinc ion at a protein concentration of approximately 2  $\mu$ M. As the protein concentration decreased, the relative peak intensity of zinc-bound *Kkr*RseP decreased, while the relative intensity of zinc-free *Kkr*RseP increased. In contrast, zinc-free *Ec*RseP ions were not observed even at 0.6  $\mu$ M.

The difference in zinc ion binding affinity between *Ec*RseP and *Kkr*RseP was also confirmed using RseP orthologs with different C-terminal sequences around the affinity tag regions, *Ec*RseP\_v2 and *Kkr*RseP\_v2 (Figure S1). As shown in Figure S3, *Ec*RseP\_v2 and *Kkr*RseP\_v2 exhibited similar zinc-binding affinity to their parent orthologs, *Ec*RseP and *Kkr*RseP, respectively, across varied protein concentrations. Specifically, *Ec*RseP\_v2 retained Zn even at 0.5  $\mu$ M, whereas zinc ions in *Kkr*RseP\_v2 were easily detached at low protein concentrations. Consequently, we can conclude that *Ec*RseP exhibits a higher zinc ion binding affinity than *Kkr*RseP.

Although the crystal structure of the RseP orthologs without inhibitor is not available, *Ec*RseP has been reported to possess higher protease activity than *Kkr*RseP [11]. The native MS data, which demonstrate that zinc is more readily dissociated from *Kkr*RseP than *Ec*RseP, are consistent with these activity assays. Furthermore, X-ray crystallography of RseP–inhibitor complexes revealed that helix TM4 in *Kkr*RseP is positioned distal to the active site, where the zinc ion resides, whereas in *Ec*RseP, it is located proximal to the

active site (Figure S4). While the TM4 positional difference might be attributed to crystallization artifacts, the native MS results support the observed structural variations. In other words, native MS provided information on the environmental differences around the zinc ions between *Ec*RseP and *Kkr*RseP.

### Inhibitor binding to RseP orthologs

We then investigated the binding of batimastat, a peptide mimetic inhibitor of *Ec*RseP (Fig. 3), to RseP orthologs using native MS. Batimastat was added to the protein solutions, and the resulting solutions were analyzed by native MS. Figures 4 and S5 present the ESI mass spectra of 1  $\mu$ M *Ec*RseP and *Kkr*RseP, both in the absence and presence of 5  $\mu$ M batimastat. Due to batimastat's limited aqueous solubility at high concentrations, it was initially dissolved in DMSO and subsequently added to the protein solutions, resulting in final concentrations of 5  $\mu$ M batimastat and 0.025% DMSO. We observed a decrease in the intensities of the 13+, 14+, and 15+ charged peaks of both *Ec*RseP and *Kkr*RseP in the presence of batimastat. It is considered that ions at higher charge states correspond to more elongated and less stable than those at lower charge states. Consequently, the formation of a stable complex with batimastat could lead to a decrease in the relative abundance, and thus, the peak intensities, of these higher charge state ions.

In the absence of batimastat, *Ec*RseP predominantly retained a zinc ion, while *Kkr*RseP largely lacked zinc at a

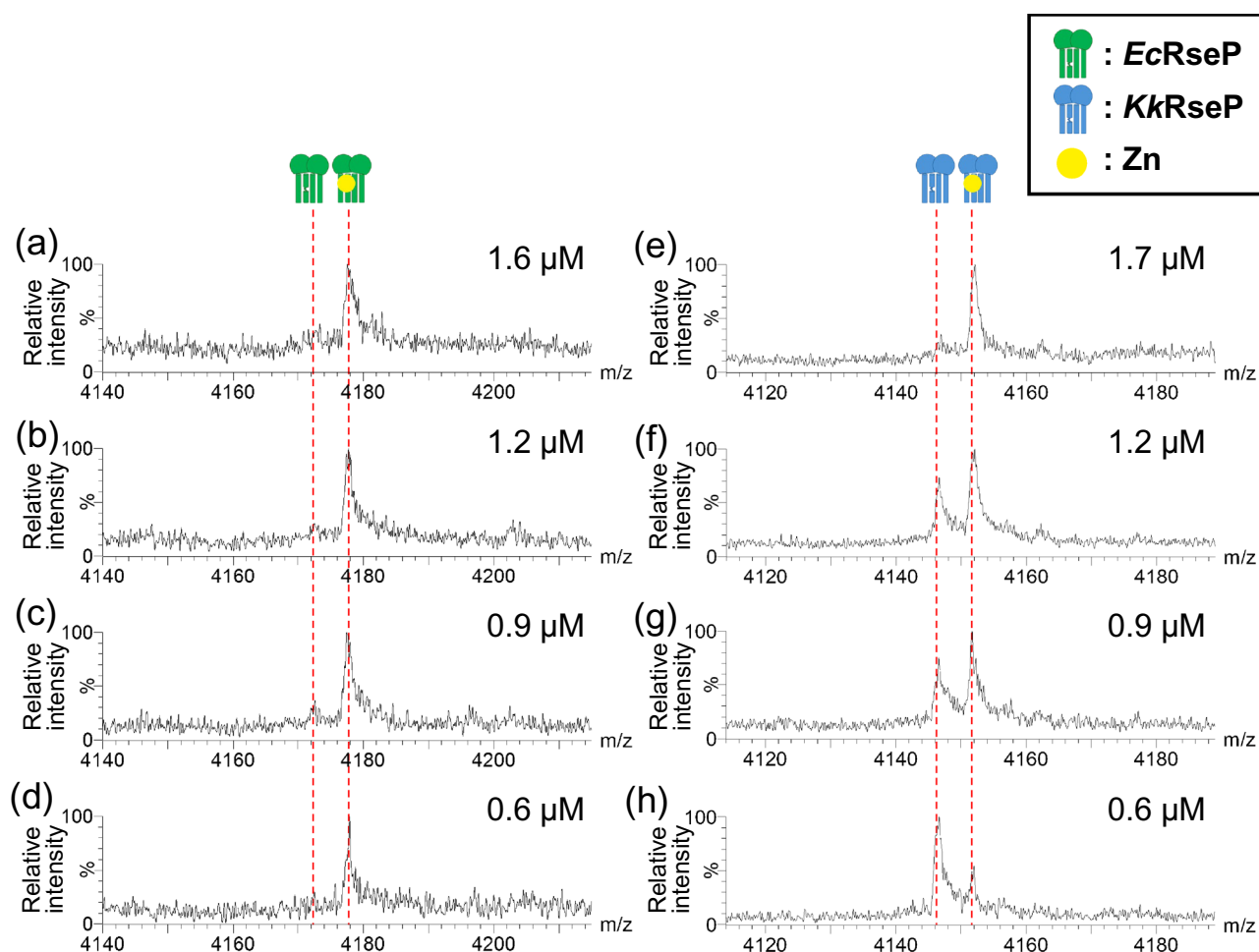


**Fig. 2** Expanded mass spectra of 12+ charged ions of 1.6 (a), 1.2 (b), 0.9 (c), and 0.6  $\mu\text{M}$  (d) *EcRseP* and 1.7 (e), 1.2 (f), 0.9 (g), and 0.6  $\mu\text{M}$  (h) *KkRseP*. Peaks of *Ec* and *KkRseP* are marked with green and blue cartoons, respectively. The yellow circle cartoon corresponds to zinc ion

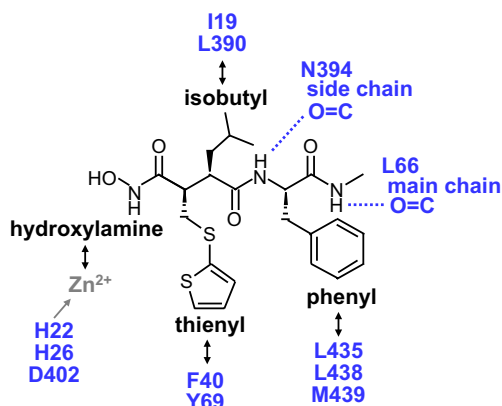


**Fig. 3** Chemical structure of batimastat. Molecular interactions between RseP and batimastat are indicated

protein concentration of 1  $\mu\text{M}$ . Upon batimastat addition, additional peaks corresponding to a 1:1 complex of RseP and batimastat, containing a zinc ion, were observed for both

orthologs. Concurrently, the peaks corresponding to zinc-free RseP nearly disappeared. These results demonstrate that batimastat binding to RseP stabilizes and promotes zinc ion coordination within the active site, and that the zinc ion is essential for batimastat binding. Notably, native MS enables such detailed investigations. The enhanced stability of both RseP orthologs, when bound to zinc and batimastat, facilitated their structure elucidation through X-ray crystallography [11].

We then investigated the stability of the RseP–batimastat complex for both RseP orthologs by varying the collision voltage in native MS experiments. Figure 5 presents the ESI mass spectra of *EcRseP* and *KkRseP* complexed with batimastat, obtained at collision voltages ranging from 30 to 50 V. As the collision voltage increased, the relative intensity of the complex decreased, indicating that hydrophobic interactions contribute to complex formation (discussed later) [28–30]. At a collision voltage of 45 V, the complex peaks nearly disappeared for both RseP orthologs. The experiments were performed in triplicate, and the average values of the relative peak intensity of the RseP–batimastat

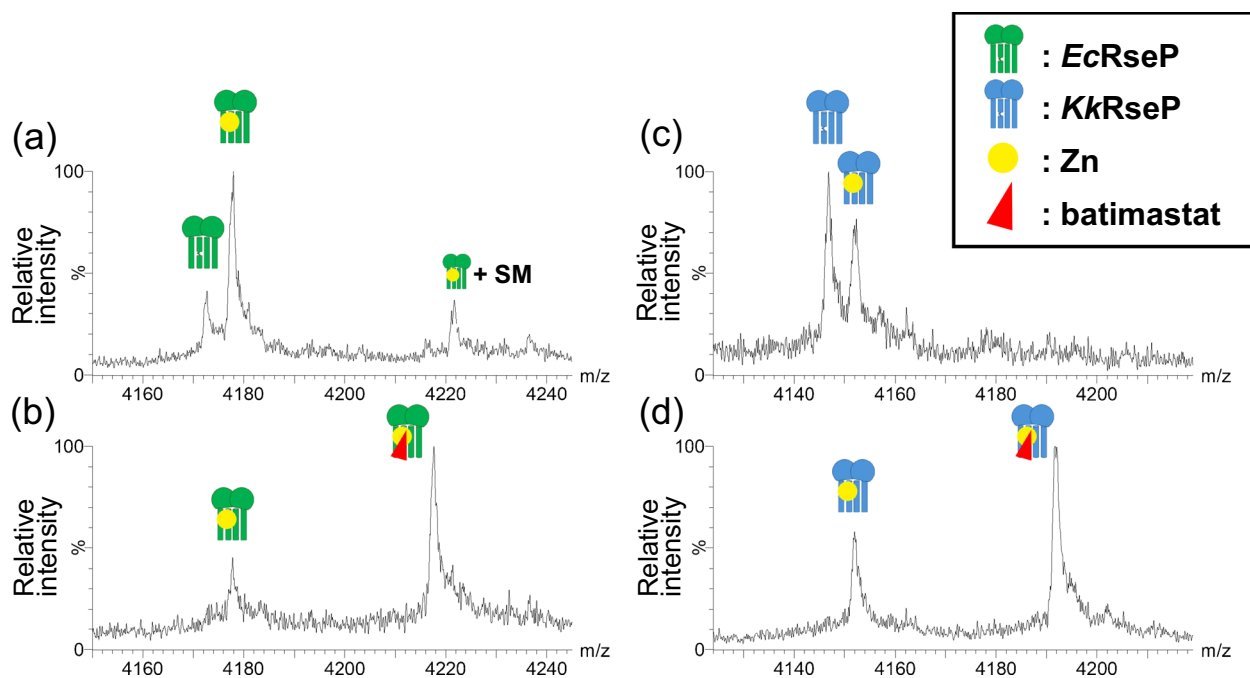


**Fig. 4** Expanded mass spectra of 12+ charged ions of *Ec* and *KkrRseP* in the absence (**a**, **c**) and presence (**b**, **d**) of batimastat. Peaks of *Ec* and *KkrRseP* are marked with green and blue cartoons, respectively.

The yellow circle and red triangle cartoons correspond to zinc ion and batimastat, respectively. In (**a**), an SM adduct to zinc-bound *EcRseP* is observed

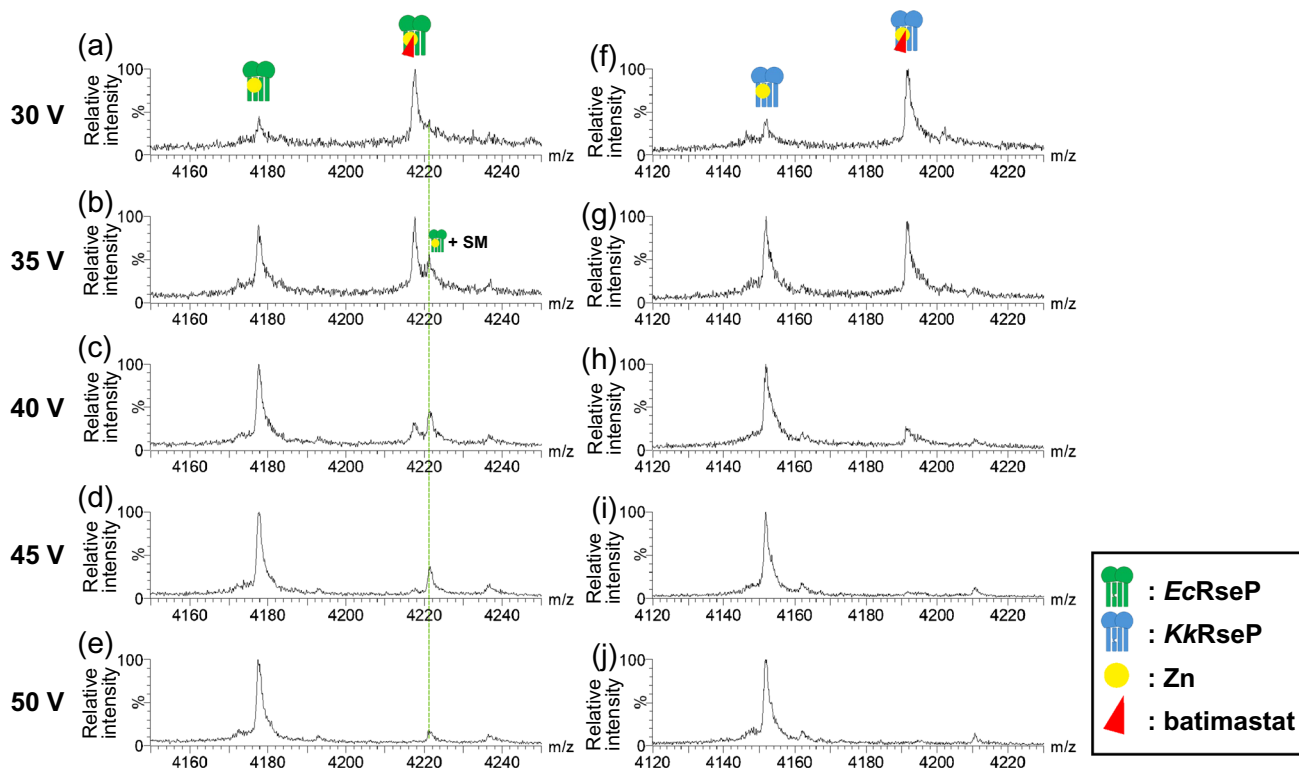
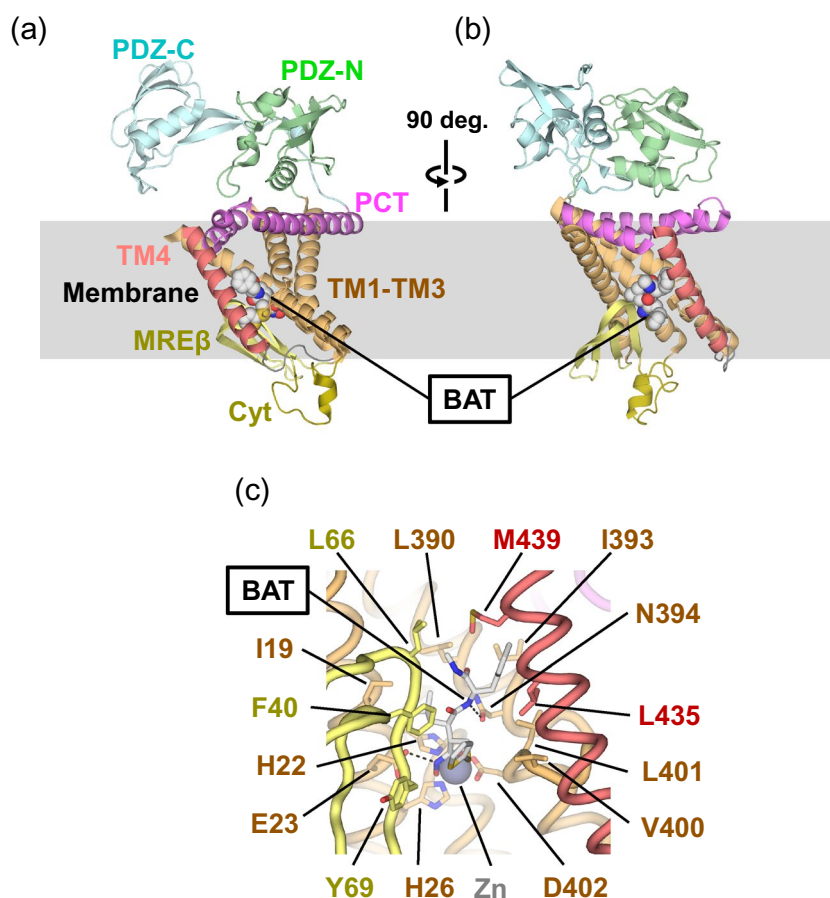


**Fig. 5** Expanded mass spectra of 12+ charged ions of *Ec* and *KkrRseP* in the presence of batimastat obtained at 30 V (**a**, **f**), 35 V (**b**, **g**), 40 V (**c**, **h**), 45 V (**d**, **i**), and 50 V (**e**, **j**) of TRAP collision voltage. Peaks of *Ec* and *KkrRseP* are marked with green and blue cartoons, respec-

tively. The yellow circle and red triangle cartoons correspond to zinc ion and batimastat, respectively. In (**a–e**), an SM adduct to zinc-bound *EcRseP* is observed

**Fig. 6** Structure of *Ec*RseP complexed with batimastat (PDB: 7W6X). (a) and (b) *Ec*RseP–batimastat complex embedded in the membrane. The batimastat molecule is indicated in the sphere models. Blue and red spheres correspond to nitrogen and oxygen atoms, respectively. (c) Enlarged structure around the batimastat molecule in (b). The batimastat molecule is indicated in the stick models. Zinc ion is indicated in a gray sphere. The amino acid residues in *Ec*RseP involved in the interaction with batimastat and zinc ion are indicated in a one-letter notation with the residue position number. Hydrogen bonds between *Ec*RseP and batimastat are indicated in dotted lines



complex ions to the total protein ion intensity were plotted against different collision voltages. As shown in Figure S6, this analysis revealed no discernible difference in the complex stability between the two orthologs.

In contrast to batimastat binding, the peak corresponding to the association of one molecule of SM, the detergent used during RseP purification, persisted even at a collision voltage of 50 V for *Ec*RseP. This observation suggests strong SM binding to *Ec*RseP, resulting in SM adducts even under conditions that disrupt batimastat binding. We confirmed that residual SM molecules were difficult to remove during MS measurements, even after solvent exchange. Conversely, adducts of DDAO molecules, which replaced SM prior to MS, were not detected in the mass spectrum. These results highlight the importance of selecting an appropriate detergent for successful observation of membrane protein–inhibitor complexes.

As demonstrated, batimastat binding stabilized the complex, enabling its detection during MS measurement under mild conditions. However, maintaining membrane protein–ligand complexes in native MS is generally challenging [21, 23, 27, 31], with successful observations of membrane protein–drug complexes remaining limited [23, 27]. Peptide drug complexes often benefit from multiple interactions, including hydrogen bonding and electrostatic forces,

facilitating their observation by native MS [27, 31, 32]. In contrast, small-molecule drug complexes, with fewer interaction sites and reliance on hydrophobic interactions within the membrane, are more difficult to preserve during MS analysis. Consequently, there have been few studies of the observation of protein–small-molecule drug complexes [23, 27, 31]. In the *Ec*RseP–batimastat complex, batimastat binds to the RseP active site within the membrane, as shown in Fig. 6. Two hydrogen bonds and several van der Waals contacts contribute to the complex stability (Figs. 3, 6, and S4) [11]. Several aliphatic amino acids, such as leucine, isoleucine, phenylalanine, tyrosine, and methionine, contribute to hydrophobic interactions with batimastat. It is likely that the cooperative effect of these van der Waals interactions and hydrogen bonds enabled successful observation of the complex.

## Conclusion

In this study, we employed native MS to characterize zinc and inhibitor binding to two RseP orthologs. In the absence of batimastat, a specific inhibitor, we observed a distinct difference in zinc affinity between the orthologs. *Kkr*RseP exhibited a greater propensity to release zinc ions than

*EcRseP* at sub-micromolar protein concentrations in native MS. Conversely, the stability of the RseP–zinc–batimastat complex did not show a significant difference between the two orthologs. Although the X-ray structures of the RseP orthologs without batimastat remain undetermined, we could observe zinc-bound RseP ions in native MS and discuss the differences in zinc affinity.

Inhibitor binding significantly stabilized the RseP complex, enabling the observation of intact complex ions under mild native MS conditions. While maintaining and observing intact membrane protein–inhibitor complexes in native MS is challenging, particularly for inhibitors that bind within the transmembrane region via hydrophobic interactions, our optimized sample preparation and measurement conditions facilitated successful observation. This study demonstrates the potential of native MS as a valuable platform for identifying drug candidates targeting membrane proteins.

**Supplementary Information** The online version contains supplementary material available at <https://doi.org/10.1007/s00216-025-06173-8>.

**Author contribution** SA and TN conceived and designed the study. MT, TS, RO, HK, and KS conducted the experimental investigation. YK provided a PA-tag system for protein purification. SA, MT, and TN analyzed the data and wrote the manuscript. SA supervised the project.

**Funding** This work was partly supported by the Japan Society for the Promotion of Science (JSPS) KAKENHI grant numbers JP19H05774, JP21K19236, JP24K0934 (to SA), JP22H02561, and JP23K23825 (to TN), Japan Agency for Medical Research and Development (AMED) under grant number JP24ama121008 (to YK), and a research grant from the Daiichi Sankyo Foundation of Life Science (to SA).

**Data availability** The data supporting the findings of this study will be made available upon request from the corresponding author.

## Declarations

**Conflict of interest** The authors declare no competing interests.

## References

- Kühnle N, Dederer V, Lemberg MK. Intramembrane proteolysis at a glance: from signalling to protein degradation. *J Cell Sci*. 2019;132:jcs217745.
- Beard HA, Barniol-Xicota M, Yang J, Verhelst SHL. Discovery of cellular roles of intramembrane proteases. *ACS Chem Biol*. 2019;14:2372–88.
- Brown MS, Ye J, Rawson RB, Goldstein JL. Regulated intramembrane proteolysis: a control mechanism conserved from bacteria to humans. *Cell*. 2000;100:391–8.
- Kanehara K, Akiyama Y, Ito K. Characterization of the yaeL gene product and its S2P-protease motifs in *Escherichia coli*. *Gene*. 2001;281:71–9.
- Kanehara K, Ito K, Akiyama Y. YaeL (EcfE) activates the sigma(E) pathway of stress response through a site-2 cleavage of anti-sigma(E). *RseA Genes Dev*. 2002;16:2147–55.
- Alba BM, Leeds JA, Onufryk C, Lu CZ, Gross CA. DegS and YaeL participate sequentially in the cleavage of RseA to activate the sigma(E)-dependent extracytoplasmic stress response. *Genes Dev*. 2002;16:2156–68.
- Saito A, Hizukuri Y, Matsuo E, Chiba S, Mori H, Nishimura O, Ito K, Akiyama Y. Post-liberation cleavage of signal peptides is catalyzed by the site-2 protease (S2P) in bacteria. *Proc Natl Acad Sci USA*. 2011;108:13740–5.
- Kroos L, Akiyama Y. Biochemical and structural insights into intramembrane metalloprotease mechanisms. *Biochim Biophys Acta*. 2013;1828:2873–85.
- Hizukuri Y, Akiyama K, Akiyama Y. Biochemical characterization of function and structure of RseP, an *Escherichia coli* S2P protease. *Methods Enzymol*. 2017;584:1–33.
- Kristensen SS, Diep DB, Kjos M, Mathiesen G. The role of site-2-proteases in bacteria: a review on physiology, virulence, and therapeutic potential. *Microbiolife*. 2023;4: uqad025.
- Imaizumi Y, Takanuki K, Miyake T, Takemoto M, Hirata K, Hirose M, Oi R, Kobayashi T, Miyoshi K, Aruga R, Yokoyama T, Katagiri S, Matsuura H, Iwasaki K, Kato T, Kaneko MK, Kato Y, Tajiri M, Akashi S, Nureki O, Hizukuri Y, Akiyama Y, Nogi T. Mechanistic insights into intramembrane proteolysis by E. coli site-2 protease homolog RseP. *Sci Adv*. 2022;8: eabp9011.
- Loo JA. Studying noncovalent protein complexes by electrospray ionization mass spectrometry. *Mass Spectrom Rev*. 1997;16:1–23.
- Ruotolo BT, Robinson CV. Aspects of native proteins are retained in vacuum. *Curr Opin Chem Biol*. 2006;10:402–8.
- Heck AJR. Native mass spectrometry: a bridge between interactomics and structural biology. *Nat Methods*. 2008;5:927–33.
- Leney AC, Heck AJR. Native mass spectrometry: what is in the name? *J Am Soc Mass Spectrom*. 2017;28:5–13.
- Takano K, Arai S, Sakamoto S, Ushijima H, Ikegami T, Saikusa K, Konuma T, Hamachi I, Akashi S. Screening of protein-ligand interactions under crude conditions by native mass spectrometry. *Anal Bioanal Chem*. 2020;412:4037–43.
- Barrera NP, Di Bartolo N, Booth PJ, Robinson CV. Micelles protect membrane complexes from solution to vacuum. *Science*. 2008;321:243–6.
- Yen HY, Jazayeri A, Robinson CV. G protein-coupled receptor pharmacology-insights from mass spectrometry. *Pharmacol Rev*. 2023;75:397–415.
- Reading E, Liko I, Allison TM, Benesch JL, Laganowsky A, Robinson CV. The role of the detergent micelle in preserving the structure of membrane proteins in the gas phase. *Angew Chem Int Ed Engl*. 2015;54:4577–81.
- Laganowsky A, Reading E, Hopper JT, Robinson CV. Mass spectrometry of intact membrane protein complexes. *Nat Protoc*. 2013;8:639–51.
- Bolla JR, Howes AC, Fiorentino F, Robinson CV. Assembly and regulation of the chlorhexidine-specific efflux pump AceI. *Proc Natl Acad Sci U S A*. 2020;117:17011–8.
- Gault J, Donlan JA, Liko I, Hopper JT, Gupta K, Housden NG, Struwe WB, Marty MT, Mize T, Bechara C, Zhu Y, Wu B, Kleanthous C, Belov M, Damoc E, Makarov A, Robinson CV. High-resolution mass spectrometry of small molecules bound to membrane proteins. *Nat Methods*. 2016;13:333–6.
- Tajiri M, Imai S, Konuma T, Shimamoto K, Shimada I, Akashi S. Evaluation of drug responses to human  $\beta_2$ AR using native mass spectrometry. *ACS Omega*. 2023;8:24544–51.
- Urner LH, Liko I, Yen HY, Hoi KK, Bolla JR, Gault J, Almeida FG, Schweder MP, Shutin D, Ehrmann S, Haag R, Robinson CV, Pagel K. Modular detergents tailor the purification and structural analysis of membrane proteins including G-protein coupled receptors. *Nat Commun*. 2020;11:564.
- Strop P, Brunger AT. Refractive index-based determination of detergent concentration and its application to the study of membrane proteins. *Protein Sci*. 2005;14:2207–11.

26. Sanchez SA, Gratton E, Zanolco AL, Lemp E, Gunther G. Sucrose monoester micelles size determined by Fluorescence Correlation Spectroscopy (FCS). *PLoS ONE*. 2011;6: e29278.
27. Liu Y, LoCaste CE, Liu W, Poltash ML, Russell DH, Laganowsky A. Selective binding of a toxin and phosphatidylinositides to a mammalian potassium channel. *Nat Commun*. 2019;10:1352.
28. Veros CT, Oldham NJ. Quantitative determination of lysozyme-ligand binding in the solution and gas phases by electrospray ionisation mass spectrometry. *Rapid Commun Mass Spectrom*. 2007;21:3505–10.
29. Liu L, Kitova E, Klassen J. Quantifying protein-fatty acid interactions using electrospray ionization mass spectrometry. *J Am Soc Mass Spectrom*. 2011;22:310–8.
30. Cubrilovic D, Biela A, Sielaff F, Steinmetzer T, Klebe G, Zenobi R. Quantifying protein-ligand binding constants using electrospray ionization mass spectrometry: a systematic binding affinity study of a series of hydrophobically modified trypsin inhibitors. *J Am Soc Mass Spectrom*. 2012;23:1768–77.
31. Bennett JL, Nguyen GTH, Donald WA. Protein-small molecule interactions in native mass spectrometry. *Chem Rev*. 2022;122:7327–85.
32. Marcoux J, Wang SC, Politis A, Reading E, Ma J, Biggin PC, Zhou M, Tao H, Zhang Q, Chang G, Morgner N, Robinson CV. Mass spectrometry reveals synergistic effects of nucleotides, lipids, and drugs binding to a multidrug resistance efflux pump. *Proc Natl Acad Sci USA*. 2013;110:9704–9709.

**Publisher's Note** Springer Nature remains neutral with regard to jurisdictional claims in published maps and institutional affiliations.

Springer Nature or its licensor (e.g. a society or other partner) holds exclusive rights to this article under a publishing agreement with the author(s) or other rightsholder(s); author self-archiving of the accepted manuscript version of this article is solely governed by the terms of such publishing agreement and applicable law.